帯域制限された波動伝達関数に関して(英文)

著者	木下 繁夫
雑誌名	国立防災科学技術センター 研究報告
巻	21
ページ	45-62
発行年	1979-03
URL	http://doi.org/10.24732/nied.00000791

Report of the National Research Center for Disaster Prevention, No. 21, March 1979

550.34.09

On a Band-Limited Wave Transfer Function

By

Shigeo Kinoshita*

National Research Center for Disaster Prevention, Japan

Abstract

Solving the wave transfer function in the closed form, the poles are investigated in a complex plane. The equal time layered model is applied for this purpose so that the predominant frequencies and the equivalent damping factors are easily obtained by making use of poles estimated. Futhermore, the statistical relations of input and output waves is discussed with the transmittancy function.

Particularly, the equivalent damping factor is distinguished between the quantity due to the diffusive damping effect and the one due to the internal damping effect. In this report, the above-mentioned wave transfer function is derived theoretically and the quantitative comparisons by making use the observed data are performed.

1. Introduction

Generally, there are two ways to construct the wave transfer function of the linear visco-elastic multi-layered half-space to vertical incident plane waves. One is where the general solution of the wave equation is separated into the forward and backward waves. The methods based on this way utilize the reflection coefficients which are determined by the wave impedance ratios and are only applied to homogeneous media. The other is where the representation for the general solution of the wave equation including the undecided constants is solved, directly, based on the boundary conditions. The former is adopted in our method.

At the expense of an unlimited frequency range which useful matrix formulations and others are able to deal with, we construct an approximate closed form of the wave transfer function of band-limited frequency range. However, in this formulation, the restriction of frequency range is insignificant in the field of earthquake engineering and the significant informations on the vibrational characteristics of surface layers on the half-space are easily extracted as compared with other methods.

To evaluate the validity of the theoretically estimated wave transfer function, the data observed earthquake waves are used. The data observed at Iwatsuki Crustal Activity observatory are applied as a test case, because the under-ground structure

* Earthquake Engineering Laboratory, Second Research Division

at this site has been well investigated.

2. Wave transfer function

Our approximation, namely, the construction of the band-limited wave transfer function, consists of adopting the so-called "equal time layered model" as shown in Fig. 1, slicing the accurate layers into thinner layers if necessary so as to make all traveltimes equal and introducing zero reflection coefficients where required. We denote this common time by T/2. Because of the common time, the maximum frequency provided for the wave transfer function is restricted by $1/2T$ and a complex variable z is defined by

$$z = \exp(i\lambda);\ \lambda=\omega T,\ |\lambda| \leq \pi, \tag{2.1}$$

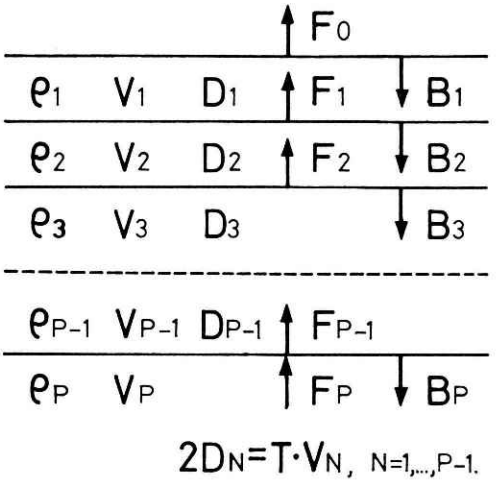


Fig. 1. Equal time layered model

where frequency parameter λ is called normalized circular frequency.

Next, we confirm some notations frequently used. Representing the wave impedance ratio between the n-th layer and the $(n+1)$-th layer as

$$\alpha_{n+1} = (\rho_n c_n / \rho_{n+1} c_{n+1})^{1/2} \tag{2.2}$$

in which c_n stands for either μ_n (S-wave) or $\lambda_n+2\mu_n$ (P-wave) and ρ_n is the density of the n-th layer, the reflection coefficient of the backward wave between the n-th layer and the $(n+1)$-th layer is as follows:

$$\beta'_{n+1} = (\alpha_{n+1} - 1)/(\alpha_{n+1} + 1). \tag{2.3}$$

Parameters μ_n and λ_n are Lame's constants for the perfectly elastic medium. Taking account of the above notations, we describe the outline for formulation, which consists of four parts, of the wave transfer function in a simple closed form.

[1] The z-transformed forward and backward waves in the n-th layer are designated by $F_n(\lambda)$ and $B_n(\lambda)$, respectively, as shown in Fig. 1. As easily shown, the waves between the n-th layer and the $(n+1)$-th layer are related by the following matrix relations

$$U_{n+1}(\lambda) = (1-\beta'_{n+1})^{-1} \cdot Q_{n+1}(\lambda) \cdot U_n(\lambda),\ n=0, 1, \cdots\cdots, p-1, \tag{2.4}$$

where

$$Q_{n+1}(\lambda) \equiv \begin{bmatrix} z^{1/2} & -\beta'_{n+1} \\ -\beta'_{n+1} & z^{-1/2} \end{bmatrix} \text{ and } U_n(\lambda) \equiv \begin{bmatrix} F_n(\lambda) \\ B_n(\lambda) \end{bmatrix}. \tag{2.5}$$

Introducing the following matrices

$$A_n(\lambda)=[a_{ij}^n(\lambda)]_{i,j=1,2}\equiv\prod_{m=1}^{n}Q_m(\lambda), \tag{2.6}$$

we know that these matrices are Hermitian and the wave transfer function is able to be represented by the elements of matrix $A_{p-1}(\lambda)$
as follows:

$$G(\lambda)\equiv F_0(\lambda)/F_p(\lambda)=\frac{\sigma_p}{a_{11}^{p-1}(\lambda)-\beta_p'\cdot z^{-1/2}\cdot a_{12}^{p-1}(-\lambda)}, \tag{2.7}$$

where $\sigma_p\equiv\prod_{n=1}^{n}(1-\beta_n')$ (2.8)

[2] The relations

$$a_{11}^n(\lambda)=z^{1/2}\cdot a_{12}^n(\lambda),\quad n=1,\ \cdots\cdots,\ p, \tag{2.9}$$

are obtained by making use of the so-called method of mathematical induction. At the same time, we have the following recursive relations

$$a_{11}^1(\lambda)=z^{1/2},\ a_{11}^n=z^{1/2}\,[a_{11}^{n-1}(\lambda)+\beta_1'\beta_n'\cdot a_{11}^{n-1}(-\lambda)],\ n=2,\cdots\cdots,p, \tag{2.10}$$

From these facts, the wave transfer function reduces to the following form

$$G(\lambda)=\frac{\sigma_p}{z^{-1/2}\cdot a_{11}^p(\lambda)}, \tag{2.11}$$

Furthermore, introducing a transformation

$$g_n(\lambda)=z^{-1/2}\cdot a_{11}^n(\lambda), \tag{2.12}$$

the wave transfer function (2.11) and the recursive relation (2.10) become

$$G(\lambda)=\frac{\sigma_p\cdot z^{-(p-1)/2}}{g_p(\lambda)} \tag{2.13}$$

and

$$g_1(\lambda)=1,\ g_n(\lambda)=g_{n-1}(\lambda)+\beta_1'\beta_n'\cdot z^{-(n-1)}\cdot g_{n-1}(-\lambda),\ n=2,\cdots\cdots,p, \tag{2.14}$$

respectively.

[3] The denominator of the wave transfer function is estimated to have the following polynomial expresion

$$g_p(\lambda)=1+\sum_{n=1}^{p-1}g_n^{p-1}\cdot z^{-n}. \tag{2.15}$$

The set of coefficients appeared in the relation (2.15) is calculated by the recursive relations (2.14). Explicit expression of the recursive relation, then, becomes

$$g_{n-1}^{n-1}=\beta_1'\beta_n',\ g_j^{n-1}=g_j^{n-2}+g_{n-1}^{n-1}\,g_{n-1-j}^{n-2},\ n=2,\cdots\cdots,p;\ j=1,\cdots\cdots,n-1. \tag{2.16}$$

Namely, we can obtain the wave transfer function by making use of relations (2.8),

(2.13), (2.15) and (2.16).

[4] Until now, we considered the wave transfer function for perfectly elastic media. To correspond to the actual situation, we must introduce the visco-elasticity of the medium. In this report, we consider the case where the type of visco-elasticity is common to all layers and the half-space. As is well known, in this case, the characteristics of visco-elasticity are introduced by performing a frequency transformation to the results obtained for the perfectly elastic case (Kobori and Minai, 1969). Two frequently used types, the constant Q type and the Voigt type, are easily applicable to our method. In these cases, Lame's constant c_n for the perfectly elastic case is transformed into $c_n \cdot q(i\lambda)$ in which

$$q(i\lambda) = \begin{cases} 1 + i/Q_e & \text{for the constant } Q \text{ type} \quad (2.17) \\ 1 + i\lambda/Q_v T & \text{for the Voigt type.} \quad (2.18) \end{cases}$$

Then, we can use

$$\lambda / \sqrt{q(i\lambda)} \quad (2.19)$$

for the visco-elastic case, instead of the frequency parameter λ for the perfectly elastic case. Furthermore, we impose the condition

$$Q_e \gg 1 \text{ and } Q_v \gg \lambda T. \quad (2.20)$$

Consequently, when the wave transfer function is evaluated, the complex variable z must be $\exp(sT)$, where

$$s \cdot T = \begin{cases} \lambda / 2Q_e + i\lambda & \text{for the constant } Q \text{ type} \quad (2.21) \\ \lambda^2 / 2Q_v T + i\lambda & \text{for the Voigt type} \quad (2.22) \end{cases}$$

in relations (2.13) and (2.15), instead of $\exp(i\lambda)$ for the perfectly elastic case.

3. Pole structure for the case where the diffusive damping effect only exists

In this section, we consider the case where the diffusive damping effect only exists. The case including the internal damping is dealt with in the next section.

A resonance phenomenon of the surface layers on the half-space is ruled by a pair of complex conjugate poles which are roots of the characteristic equation

$$g(z) \equiv g_p(-i \cdot \ln(z)) = 0 \quad (3.1)$$

in the complex z-plane. First, we consider a method for obtaining the predominant frequency and the equivalent damping factor or the $-3dB$ bandwidth. Describing a pair of complex conjugate poles of characteristic equation (3.1) as

$$r \cdot \exp(\pm i\theta), \quad (3.2)$$

the predominant frequency F and the -3dB bandwidth B are easily estimated in contrast to the representation of a pair of complex conjugate poles for the second order

system, namely,

$$\exp(-\pi B T)\cdot\exp(\pm i 2\pi F T). \tag{3.3}$$

Consequently, we obtain

$$F=\theta/2\pi T,\quad B=-1\mathrm{n}(r)/\pi T \text{ and } h=B/2F=-1\mathrm{n}(r)/\theta, \tag{3.4}$$

where parameter h is the equivalent damping factor and $|r|<1$ is the condition by which the stability of the wave transfer function is granted. The reciprocal of πB is the time constant of the impulse response envelope due to the corresponding complex conjugate poles.

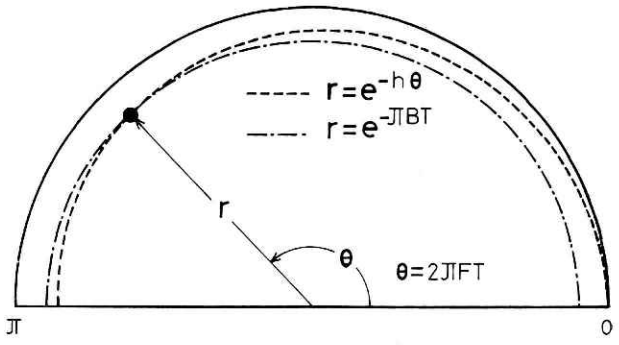


Fig. 2 Diagram of pole structure

According to the above-mentioned results, we can draw a general diagram, which is provided by the parameter T, as shown in Fig. 2. In the half circle with radius of one, we know the predominant frequencies based on the first relation in (3.4). Also, we use the spiral curves with parameter h in order to know the equivalent damping factors and the concentric semicircles with parameter B in order to know the -3dB bandwidths which are represented by

$$r=\exp(-h\theta) \tag{3.5}$$

and

$$r=\exp(-\pi B T) \tag{3.6}$$

respectively.

4. Pole structure including internal damping

As mentioned in section two, we restrict the consideration to the case where the type of visco-elasticity is common to all the layers and the half-space. To obtain the pole structure in this case, we use a well known fact that the singular points of the wave transfer function for the perfectly elastic case treated in the previous section are transformed into the corresponding ones for the visco-elastic case by making use of an inverse transformation of the relation

$$\Lambda=\lambda/\sqrt{q(i\lambda)} \tag{4.1}$$

which is approximated by the conditions (2.20) as follows:

$$\lambda=\begin{cases}\Lambda(1+i/2Q_e) & \text{for the constant } Q \text{ type} \quad (4.2)\\ \Lambda(1+i\Lambda/2Q_vT) & \text{for the Voigt type} \quad (4.3)\end{cases}$$

Consequently, a pole (3.2) for the perfectly elastic case is transformed into

$$R(\Theta)\cdot\exp(i\Theta),\quad \Theta=\Lambda, \tag{4.4}$$

where

$$R(\Theta)=\begin{cases} r\cdot\exp(-\Theta/2Q_e) & \text{for the constant } Q \text{ type} \quad (4.5)\\ r\cdot\exp(-\Theta^2/2Q_vT) & \text{for the Voigt type} \quad (4.6)\end{cases}$$

In these cases, the predominant frequencies are invariant to the perfectly elastic case. Namely, the phase of the pole is the same as the frequency parameter λ and Λ. Therefore, the diagram introduced in the previous section is also used when changing the radius r into $R(\theta)$.

From these considerations, we conclude the important result that the equivalent damping factor would be distinguished by the part due to the diffusive damping effect, namely,

$$h_d\equiv-\ln(r)/\theta, \tag{4.7}$$

and the one due to the internal damping effect, namely,

$$h_i\equiv\begin{cases} 1/2Q_e & \text{for the constant } Q \text{ type} \quad (4.8)\\ \theta/2Q_vT & \text{for the Voigt type} \quad (4.9)\end{cases}$$

The -3dB bandwidth would be also distinguished in a similar manner.

5. Wave transmittancy function

We consider the wave transmittancy function which is sometimes called the system function, which is defined by

$$S(\lambda)\equiv|G(\lambda)|^2,\quad |\lambda|\leq\pi. \tag{5.1}$$

From the definition of the wave transfer function, the reciprocal of transmittancy function is expressed by a finite Fourier cosine expansion as follows:

$$S^{-1}(\lambda)=a_0+2\sum_{n=1}^{p-1}a_n\cos(n\lambda),\quad |\lambda|\leq\pi, \tag{5.2}$$

where the coefficients $\{a_k\}_{k=1}^{p-1}$ are obtained by

$$a_k=\frac{1}{2\sigma_p^2}\cdot\sum_{n=k}^{p-1}g_{n-k}^{p-1}g_n^{p-1},\quad g_0^{p-1}=1,\ K=0,\ 1,\ \cdots\cdots,\ p-1. \tag{5.3}$$

Generally, in the case including the internal damping such as the constant Q type or the Voigt type, these coefficients are dependent on frequency and agree with the corresponding ones in the case of the diffusive dampind effect only at zero frequency.

Relation (5.2) is useful to estimate an autocorrelation function of input random process, assuming that the wave transfer function and an autocorrelation function of output random process are known. Such an estimation will be applied to know

the statistical characteristics of basement motion. Now, we denote the input and output spectral density function by $f_x(\lambda)$ and $f_v(\lambda)$, respectively. Then, an autocorrelation function of input random process is estimated by using Wiener-Khintchine's relation and relations (5.2) as follows:

$$\begin{aligned} R_v(k) &= \int_{-\pi}^{\pi} f_v(\lambda) \cdot \cos(k\lambda)\, d\lambda \\ &= \int_{-\pi}^{\pi} f_x(\lambda) \cdot S^{-1}(\lambda) \cdot \cos(k\lambda)\, d\lambda \\ &= a_0 \cdot R_x(k) + \sum_{n=1}^{p-1} a_n [R_x(k-n) + R_x(k+n)], \quad k=0,1,\cdots\cdots,p-1 \end{aligned} \tag{5.4}$$

where

$$R_x(k) = \int_{-\pi}^{\pi} f_x(\lambda) \cdot \cos(k\lambda)\, d\lambda, \quad k=0,1,\cdots\cdots,p-1, \tag{5.5}$$

are an autocorrelation function of output random process. The power spectral density function of input random process by making use of the above-obtained autocorrelation function is easily estimated. For example, the method of autoregressive model fitting is effective.

Next, we consider the mean-squared value of output process in the case of white noise input whose spectral density is $1/2\pi$. Then, the mean-squared response σ^2 is calculated by

$$\sigma^2 = \frac{1}{2\pi} \int_{-\pi}^{\pi} S(\lambda)\, d\lambda = \sigma_p^2 \cdot \sigma_0^2, \tag{5.6}$$

where σ_0^2 is the integrated value of

$$|g(z)|^{-2} = |g_p(-i \cdot \ln(z))|^{-2}$$

once around the unit circle, as follows:

$$\sigma_0^2 = \frac{1}{2\pi i} \oint \frac{1}{g(z) \cdot g(z^{-1})} \frac{dz}{z} \tag{5.7}$$

In order to evaluate σ_0^2, we use a simple method instead of using the exlpicit expressions for the residues (Jury, 1964). Namely, defining a (p,p) matrix

$$\Psi = [\psi_{ij}]_{i,j=1}, \quad \cdots\cdots p, \tag{5.8}$$

where

$$\psi_{1j} = g_{j-1}^{p-1}, \quad j = 1, \cdots\cdots, p,$$

and

$$\psi_{ij} = g_{j-i}^{p-1} + g_{i+j-2}^{p-1}, \quad i = 2, 3, \cdots\cdots, p; j = 1, 2, \cdots\cdots, p,$$

σ_0^2 is calculated by

$$\sigma_0^2 = \frac{\det(\Psi_1)}{\det(\Psi)}, \tag{5.9}$$

where Ψ_1 is a (p,p) matrix formed from Ψ by replacing the first column by the $(p,1)$ matrix whose transpose is $[1,0,0,\ldots,0,0]$. The wave transmittancy function prescribes the fraction of energy to be transmitted through the surface layers on the half-space at the various frequencies. Therefore, the parameter σ^2 shows the average energy to be transmitted through the system in normalized circular frequency $|\lambda| \leq \pi$.

6. Examples

Knowing the applicability of the results obtained in the previous sections, we test the applicability to the acceleration data observed at Iwatsuki Crustal Activity Observatory. Fig. 3 shows measurement system adopted at this site. For the accelerations gauged at GL-1m and GL-108m, the measurement with the gain response as shown in Fig. 4 has been used. Also, Fig. 5 shown the gain response at the output of F.M. transmition used for obtaining the accelerations at the base of deep-hole with the depth of 3.5km. Fig. 6 and Fig. 7 show the velocity structure proposed at the site and used for examples [1] and [2], respectively. Fig. 7 was reported by Yamamizu and Goto (1978).

[1] As the first step, we have done to compare the method of band-limited wave transfer function with Haskell's matrix method which is frequently used, for vertical incident S-wave. Surface layers used as an example is the one between ground surface and GL-108m. Fig. 8 shows a result, in which T=0.01, 0.02 and 0.03 sec are used for the calculation of band-limited wave transfer functions. These common times are corresponding to the upper limit frequencies 50, 25 and 16.7 hertz, respectively. In the case of T=0.02 sec, the method of band-limited wave transfer function shows good coincidence with the Haskell's method in the frequency range from 0 to 10 hertz. Therefore, we used the case of T=0.02 sec.

Estimating the wave transfer function using the data observed, we used the acceleration data observed at Iwatsuki GL-1m and GL-108m for the Off Miyagi Pref. earthquake (NS-component; June 12, 1978), which are shown in Fig. 9. For the main part of this record, a running coherency was obtained as shown in Fig. 10. This shows that the frequency which has meaning for estimating the wave transfer function is at most 7 hertz. Fig. 11 shows the gain curves calculated with common time T=0.02 sec and the gain estimated from the above data. The estimation of gain based on the observed data, is done by using the method of power spectrum, because this method moderately smooths the gain function compared with the statistical method which makes use of the spectral density matrix. Namely, except for the neighbourhoods of predominant frequencies, the coherency spectrum is too small to estimate smoothly the wave transfer function using the spectral density matrix. For the estimation

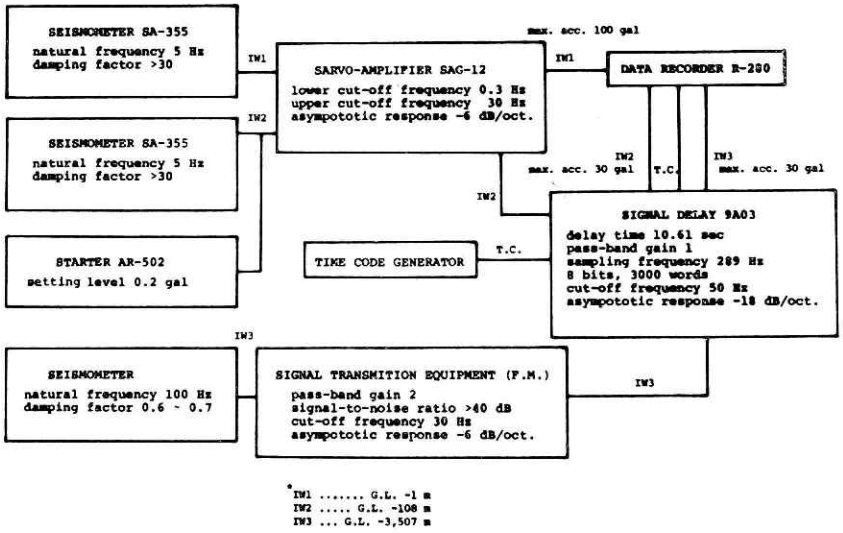


Fig. 3 Measurement system adopted at Iwatsuki Crustal Activity Observatory

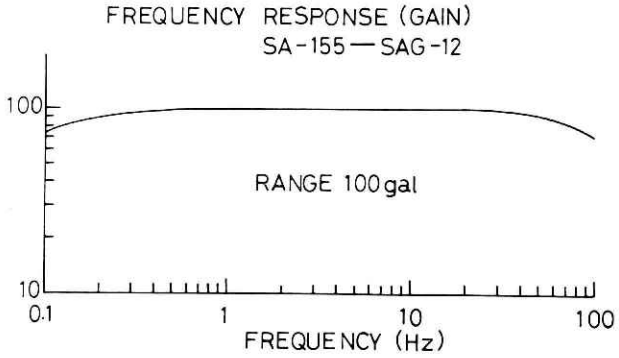


Fig. 4 Gain response adopted for shallow bore-hole

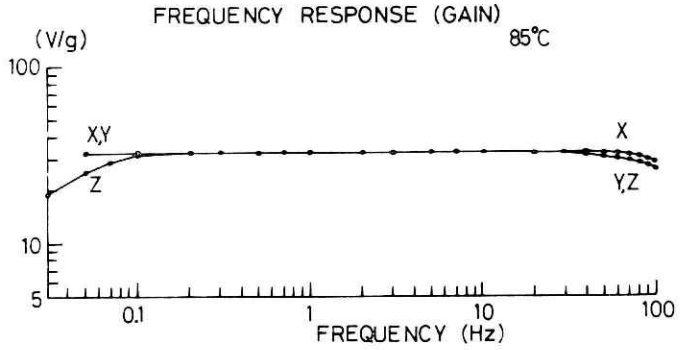


Fig. 5 Gain response adopted for deep bore-hole

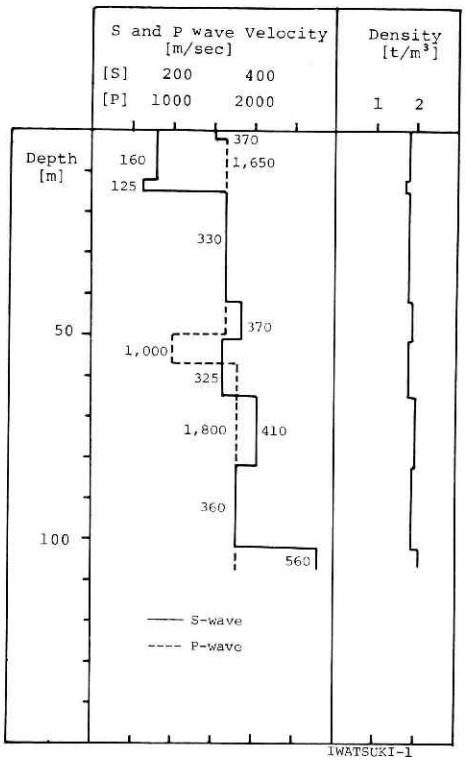


Fig. 6 Velocity structure (1)

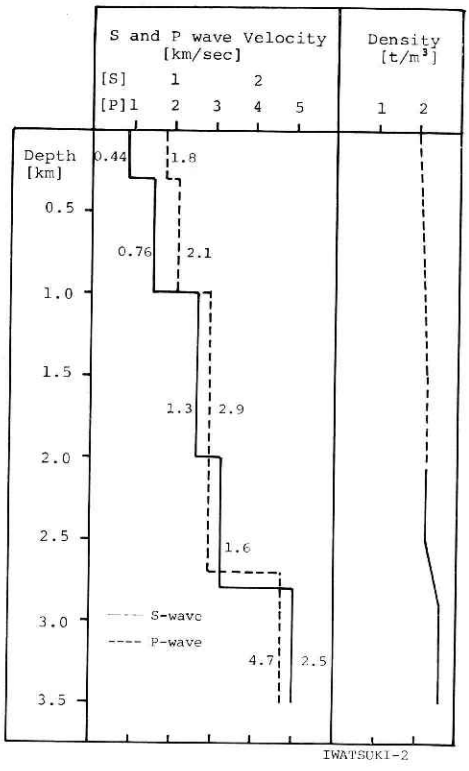


Fig. 7 Velocity structure (2) (after Yamamizu and Goto (1978))

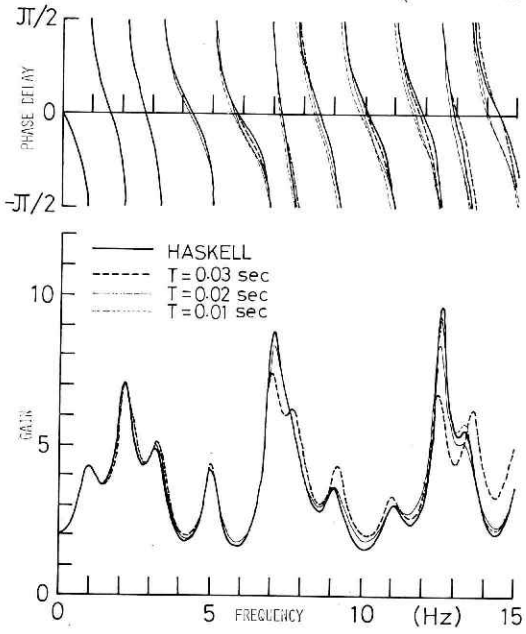


Fig. 8 Comparison between the Haskell's method and the band-limited wave transfer functions

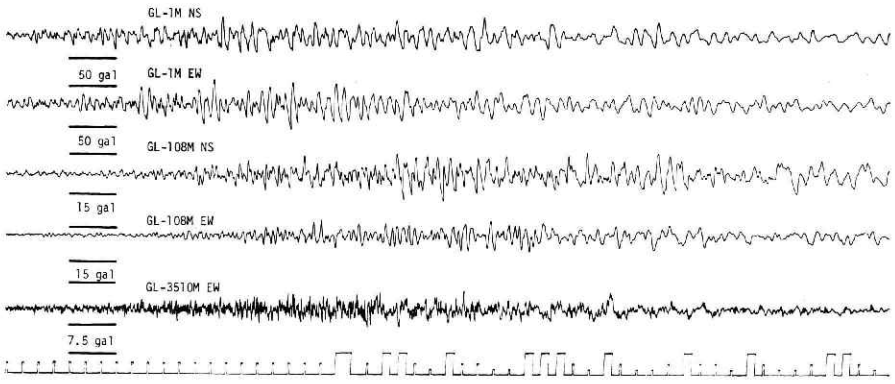


Fig. 9 Waveforms used for the example [1]

shown in Fig. 11, the frame time used is 10 seconds and the sampling time is 0.02 second. From this figure, we guess the value of Q_e as about 30 in the frequency range from 0 to 7 hertz.

Making use of relations (4.7), (4.8) and (4.9), we can apprehend the contents of the equivalent damping factors. Namely, we obtain Figs. 12, 13 and 14. In Fig. 12, the equivalent damping factors are expressed by the open circles, which indicate the case considered only the diffusive damping, and by the colsed circles, which indicate the case including the internal damping effect. For above-mentioned both cases, a tendency that the equivalent damping factors become smaller increasing

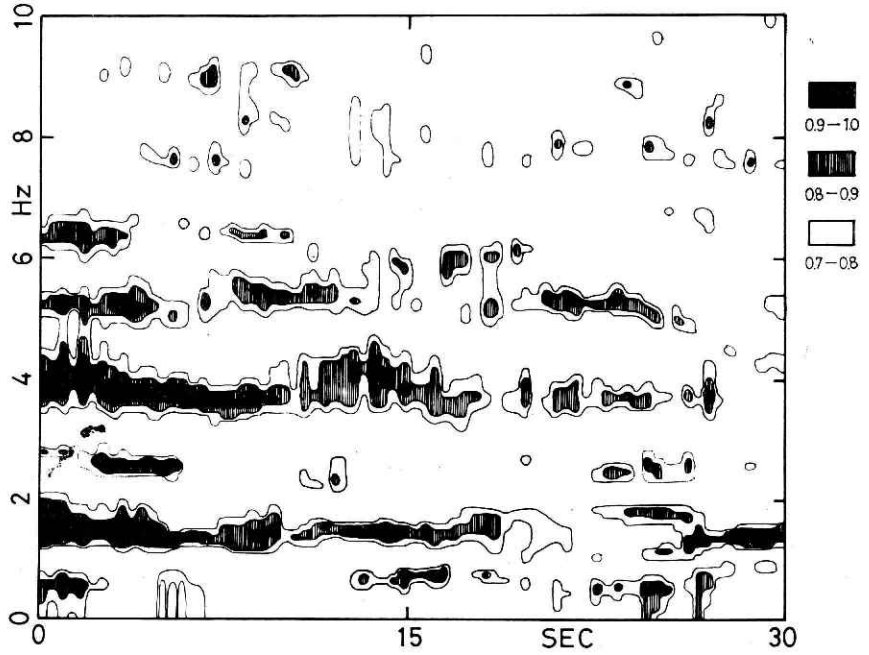


Fig. 10 Running coherency

the orders of pole, is seen. Also, Fig. 13 shows the ratios of the part occupied by the diffusive damping effect to the equivalent damping factor including the internal damping effect. From this figure, we can see that the equivalent damping facter is mainly due to the diffusive damping effect in this frequency range treated, and the percentage of the quantity due to the internal damping effect increases in proportion to frequency.

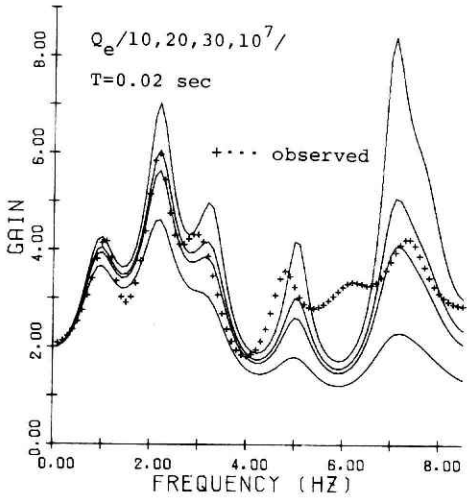


Fig. 11-1 Gains estimated for the wave transfer function at Iwatsuki GL-1m/GL-108 m for S-wave (constant Q type)

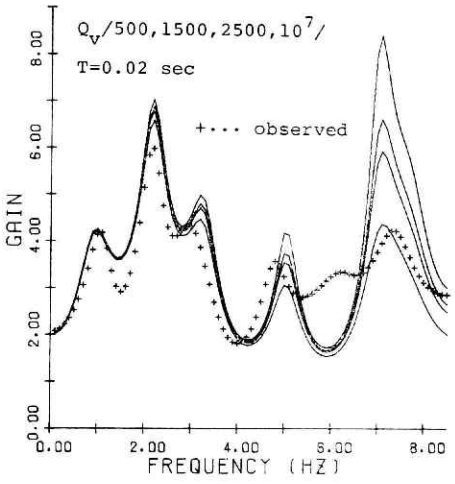


Fig. 11-2 Gains estimated for the wave transfer function at Iwatsuki GL-Im/GL-3.5 km for S-wave (Voigt type)

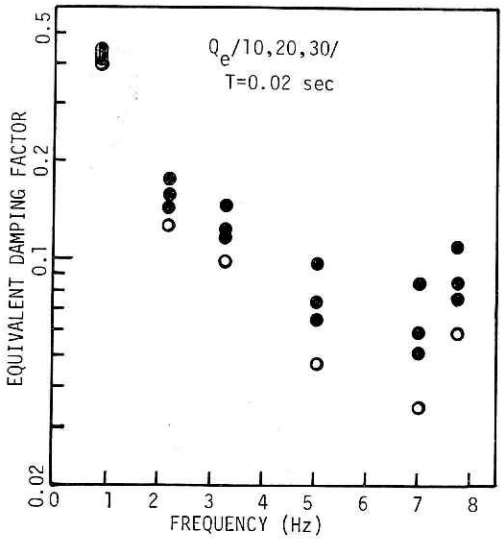


Fig. 12-1 Equivalent damping factors estimated (constant Q type)

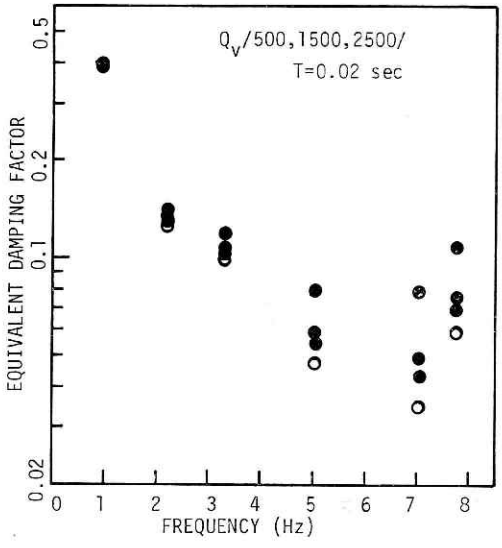


Fig. 12-2 Equivalent damping factors estimated (Voigt type)

Similary, the reciprocal of the −3dB bandwidths are shown in Fig. 14. In the case of Q_e=30, the closed circles are almost flat, indicating, and therefore, the time constants of the impulse response envelope of the corresponding poles do not differ remarkably. Finally, the diagram as shown in Fig. 15 provides an overall representation of the pole structure.

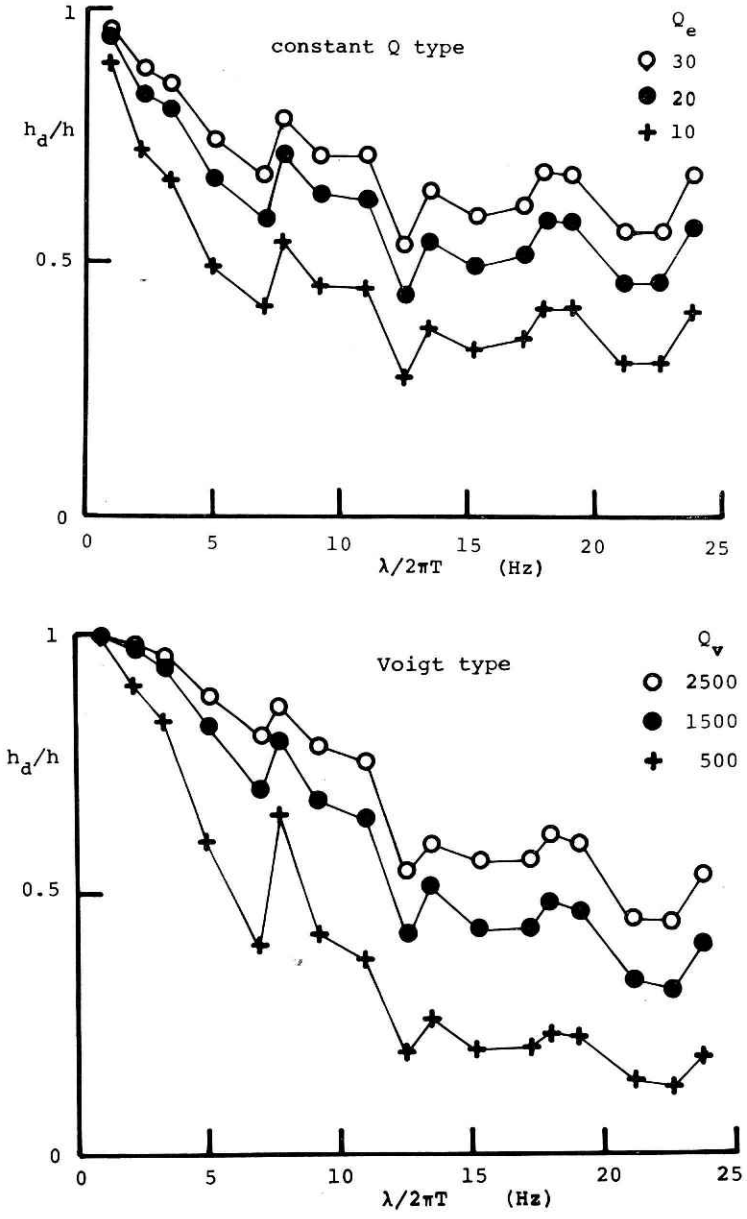


Fig. 13 Ratios of the part due to the diffusive damping effect to the equivalent damping factors

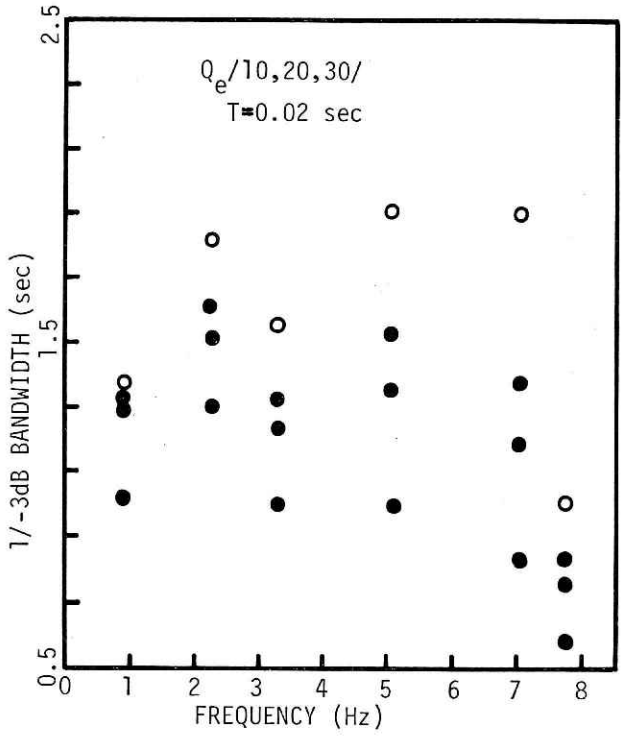


Fig. 14-1 Reciprocal of -3dB bandwidths estimated (constant Q type)

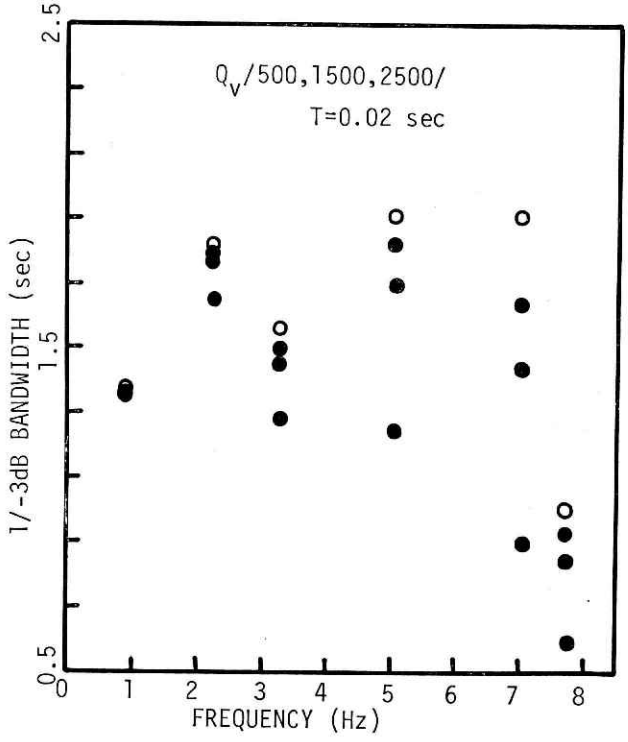


Fig. 14-2 Reciprocal of -3dB bandwidth estimated (Voigt type)

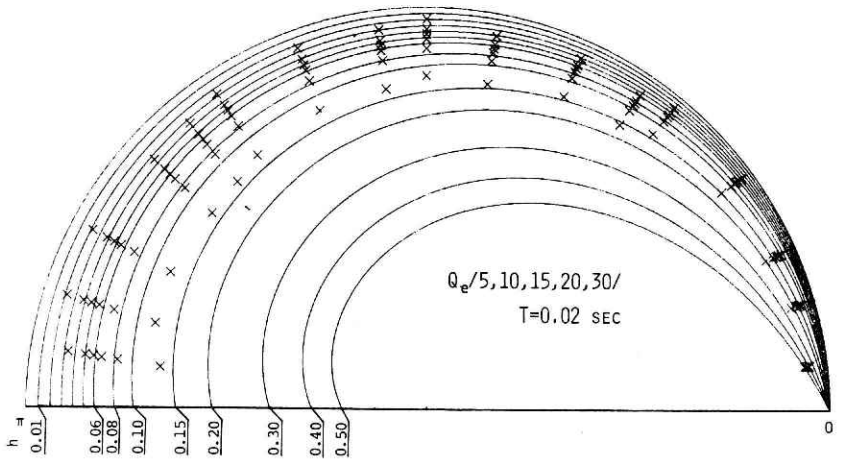


Fig. 15-1 Overall representation of pole structure (constant Q type)

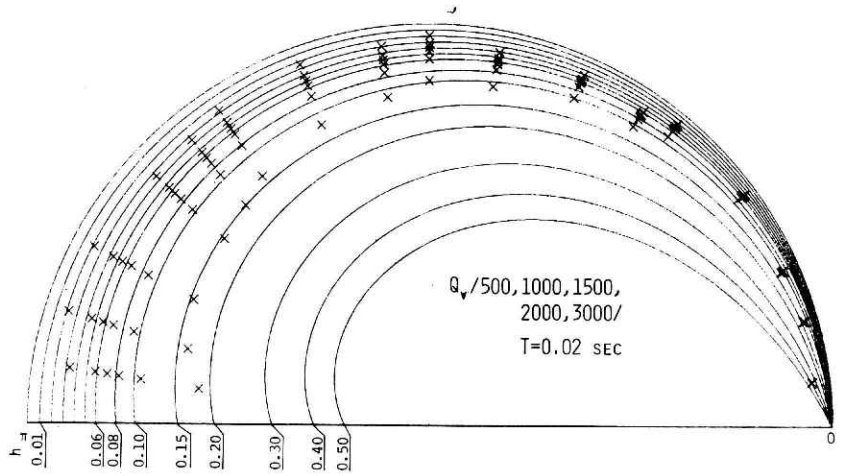


Fig. 15-2 Overall represent ation of pole structure (Voigt type)

[2] Next, we consider the effect of the surface layers on the basement using the velocity structure shown in Fig. 7. As done in the previous example, we estimate the gain of the wave transfer function by making use of acceleration data (EW-component; March 7, 1978) observed at Iwatsuki GL-1m and GL-3.5km as shown in Fig. 16. The seismic center of this shock was Off Tokai having a depth of about 400 km and magunitude of 7.8 on the J.M.A. scale. We used the data after lowpass filtering with a cutoff frequency of 1.12 hertz (—40dB/oct.) for the original shock waves.

The frequency response function estimated is shown in Fig. 17. The frame time used in the estimation is 30 seconds and the sampling time is 0.4 second. However, it is difficult to discuss the damping effect in detail based on these results estimated

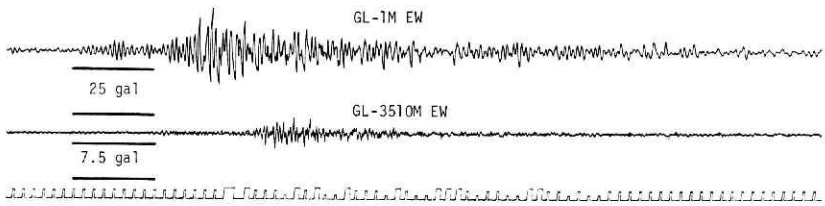


Fig. 16 Waveforms used for the example [2]

as was done in the previous example. Neverthless, the velocity structure of the *S*-wave for the surface layers and the basement at Iwatsuki which is reported, supports the peaks of the gain estimated in the period range from 2 to 10 second. In Fig. 16 as same as Fig. 9, the waves observed at GL-1m go ahead by 10.61 second compared with the othes waves and the time code.

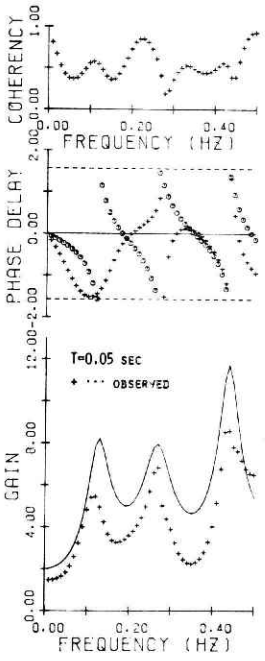


Fig. 17 Frequency response function estimated and wave transfer function at Iwatsuki GL-1m / GL-3.5 km for S-wave

7. Conclusion

A band-limited one-dimensional wave transfer function of the linear visco-elastic multi-layered half-space to vertical incident body waves is considered and applied to the acceleration data observed at Iwatsuki Crustal Activity Observatory. As the results, the following five concluding remarks are obtained.

[1] For the perfectly elastic case, the wave transfer function becomes a rational function of a complex variable $z=\exp(i\lambda)$, $|\lambda| \leq \pi$. The frequency parameter $\lambda=\omega T$ is the normalized circular frequency and a common time T is introduced by adopting the equal time layered model. The predominant frequencies and equivalent damping factors are easily estimated from the complex conjugate poles of the chracteristic eqation related to the wave transfer function in the complex z-plane.

[2] In the case where the type of visco-elasticity is commom to all the layers and the half-space, the poles obtained for the perfectly elastic case are transformed into the corresponding ones for the visco-elastic case by making use of a frequency transformation. Therefore, the quantity of pole's movement owing to the frequency transformation distinguishs the part due to the internal damping effect for the equivalent damping factor from the part due to the diffusive damping effect.

[3] The reciprocal of the transmittancy function is expresed by a finite Fourier

cosine expansion, whose expansion coefficients are obtained from the sequence of the wave impedances. Making use of these Fourier coefficients, the statistical characteristics of input random process, namely, baserock motion, is easily estimated, assuming the input and output are second order stochastic processes.

[4] A wave transfer function for S-wave at Iwatsuki GL-1m/GL-108m is estimated by making use of the acceleration data of the Off Miyagi Pref. earthquake (June 12, 1978). Estimated running coherency shows the effective upper frequency is about 7 Hz. For the constant Q model having $Q_e=30$, the ratio of the part due to the diffusive damping effect to the equivalent damping factor shows a tendency of decreasing with the orders of poles and becomes about 75% for the fouth pole having the predominant frequency of 5 Hz, Therefore, a tendency admitted generally that the more the orders of poles increase, the more the equivalent damping factors decrease, is mainly owing the diffusive damping effect in this frequency range.

[5] Making use of the acceleration data observed at Iwatsuki GL-1m and GL-3.5km, a wave transfer function for S-wave is estimated. The seismic center of the record used (March 7, 1978) is Off Tokai having a depth of about 400 km and a magnitude of 7.8 on the J.M.A. scale and Pre-Tertiary basement is assumed as the input baserock for this estimation. In the period range from 2 to 10 seconds, the peaks of gain estimated coincide with the ones of the theoretical gain obtained by making use of the velocity structure investigated by Yamamizu and Goto (1978).

References

(1) Jury, E.I. (1964): Theory and application of the Z-transform method, John-Wiley & Sons.

(2) Kobori, T. and R. Minai (1969): One-dimensional wave-transfer functions of linear viscoelastic multi-layered half-space. *Bull. Disas. Prev. Res. Inst. Kyoto Univ.*, Vol. **18.**

(3) Yamamizu, F. and N. Goto (1978): Direct measurement of seismic velocities in deep soil deposits. Proceedings of The Japan Earthquake Engineering Symposium 1978.

(Manuscript received Dec. 8, 1978)

帯域制限された波動伝達関数に関して

木 下 繁 夫

国立防災科学技術センター第二研究部耐震実験室

等方均質な粘弾性水平多層地盤に垂直入射する実体波を対象として，帯域制限された一次元波動伝達関数を考察し，岩槻で観測された加速度記録への適用を試みた．結果として，下記五項目を得た．

(1) 完全弾性体の場合，一次元波動伝達関数は，複素変数 $z=\exp(i\lambda)$，($|\lambda|\leqslant\pi$) の有理関数型表現となる．卓越振動数及び等価減衰定数は，伝達関数の特性方程式を解くことより直接推定出来る．

(2) 全ての層と入力基盤の粘弾性特性が共通であると仮定すれば，完全弾性地盤に対して得られた極構造は，周波数変換を行うことにより，粘弾性地盤の極構造へ変換される．従って，内部減衰が等価減

衰定数に占める量は，極の変換された量に対応し，逸散減衰による量から分離される．

(3) 系関数の逆数は，波動インピーダンス比の列から得られる係数列を使って，有限・フーリェ・コサイン展開される．このフーリェ係数を使うことによって，入力の統計的性質，すなわち，基盤地震動の統計的性質，が容易に推定される．ただし，入出力は，ともに二次の定常確率過程とし，出力過程の二次統計量を仮定する．

(4) 1978 年宮城県沖地震における，岩槻での観測加速度記録を用いて，この観測点での S 波伝達関数を推定した．入力基盤は地下 102m 以下としている．推定されたランニング・コヒーレンシイから，有効な推定周波数の上限は 7 Hz 程度であった．$Q=30$ の等Q型減衰の波動伝達関数でモデル化した場合，逸散効果が等価減衰定数に占める割合は極の次数の増加に伴い減衰する傾向を示すが，約 5 Hz の卓越振動数を持つ第 4 番目の極においても約75% を占めている．それ故，一般的に言われている等価減衰定数の高次減少性は主として逸散効果によるものであろう．ただし，確認出来た周波数範囲の上限はせいぜい 5 Hz 程度であり，これ以外の領域における考察は今後の課題である．特に，モデル・フリーの伝達関数推定には限界があり，今後，有理関数の係数推定を最尤法等を用いて検討する予定である．

(5) 1978 年 3 月 7 日に発生した，東海沖の深発地震（深さ 400 km，マグニチュード 7.8）の岩槻での観測加速度記録を用いて，入力基盤を先第三系の基盤とするS波伝達関数を推定した．やや長周期領域の 2～10秒の範囲内で，推定された利得のピーク周波数は，山水・後藤 (1978) によって報告されているS波速度構造を使って求めた波動伝達関数の利得のピーク周波数と一致した．